

20-Gbps WDM-PON transmissions employing weak-resonant-cavity FPLD with OFDM and SC-FDE modulation formats

I-Cheng Lu,¹ Chia-Chien Wei,^{2,*} Wen-Jr Jiang,¹ Hsing-Yu Chen,^{1,3} Yu-Chieh Chi,⁴
Yi-Cheng Li,⁴ Dar-Zu Hsu,^{1,3} Gong-Ru Lin,^{4,5,6} and Jyehong Chen¹

¹Department of Photonics, National Chiao-Tung University, Hsinchu, Taiwan, 300

²Department of Photonics, National Sun Yat-sen University, Kaohsiung, Taiwan, 804

³Information and Communications Research Labs, Industrial Technology Research Institute, Hsinchu, Taiwan, 310

⁴Graduate Institute of Photonics and Optoelectronics, National Taiwan University, Taipei, Taiwan, 106

⁵Department of Electrical Engineering, National Taiwan University, Taipei, Taiwan, 106

⁶grlin@ntu.edu.tw

*ccwei@mail.nsysu.edu.tw

Abstract: Using a colorless weak-resonant-cavity (WRC) FPLD injected by a centralized light source, we have experimentally demonstrated a superior performance of 20-Gbps uplink transmission in a WDM-PON. Even though the typical modulation bandwidth of a WRC-FPLD is only ~1.25 GHz, using spectrally-efficient 32-QAM OFDM or SC-FDE modulation, 20-Gbps uplink signals can achieve the FEC limit after 25-km dispersion-uncompensated single-mode fiber transmission. Because of the advantage of lower PAPR, the SC-FDE signals outperform the OFDM signals with the fixed 32-QAM format in the proposed system; moreover, SC-FDE scheme can be another promising candidate for uplinks in WDM-PONs, for its simplification to ONUs. The signal at the mode of 1560.7 nm shows similar quality with the signal at the modes of 1545.3 nm and 1574.7 nm, the WRC-FPLD, accordingly, has wide injection wavelength range from at least 1545.3 nm to 1574.7 nm. With the mode spacing of 0.55 nm, consequently, we have demonstrated the applicability of the colorless WRC-FPLD on supporting up to 36 channels in the WDM-PON.

©2013 Optical Society of America

OCIS codes: (060.4080) Modulation; (060.2330) Fiber optics communications; (140.3520) Lasers, injection-locked.

References and links

1. F. J. Effenberger, "The XG-PON system: cost effective 10 Gb/s access," *J. Lightwave Technol.* **29**(4), 403–409 (2011).
2. N. Cvijetic, M. Cvijetic, M. F. Huang, E. Ip, Y. K. Huang, and T. Wang, "Terabit Optical access networks based on WDM-OFDMA-PON," *J. Lightwave Technol.* **30**(4), 493–503 (2012).
3. K. Y. Cho, U. H. Hong, Y. Takushima, A. Agata, T. Sano, M. Suzuki, and Y. C. Chung, "103-Gb/s long-reach WDM PON implemented by using directly modulated RSOAs," *IEEE Photon. Technol. Lett.* **24**(3), 209–211 (2012).
4. L. Xu, Q. Li, N. Ophir, K. Padmaraju, L. W. Luo, L. Chen, M. Lipson, and K. Bergman, "Colorless optical network unit based on silicon photonic components for WDM PON," *IEEE Photon. Technol. Lett.* **24**(16), 1372–1374 (2012).
5. K. Y. Cho, Y. Takushima, and Y. C. Chung, "10-Gb/s operation of RSOA for WDM PON," *IEEE Photon. Technol. Lett.* **20**(18), 1533–1535 (2008).
6. P. Chanclou, F. Payoux, T. Soret, N. Genay, R. Brenot, F. Blache, M. Goix, J. Landreau, O. Legouezigou, and F. Mallécot, "Demonstration of RSOA-based remote modulation at 2.5 and 5 Gbit/s for WDM PON," in *Optical Fiber Communication Conference*, OSA Technical Digest (Optical Society of America, 2007), paper OWD1.
7. N. Kashima, "Injection-locked Fabry-Pérot laser diode transmitters with semiconductor optical amplifier for WDM-PON," *J. Lightwave Technol.* **27**(12), 2132–2139 (2009).

8. H. L. Zhang, G. W. Pickrell, Z. Morbi, Y. Wang, M. Ho, K. A. Anselm, and W.-Y. Hwang, "32-channel, injection-locked WDM-PON SFP transceivers for symmetric 1.25 Gbps operation," in *Optical Fiber Communication Conference*, OSA Technical Digest (Optical Society of America, 2011), paper NTuB4.
9. S. H. Yoo, H. K. Lee, D. S. Lim, J. H. Jin, L. Byun, and C. H. Lee, "2.5-Gb/s broadcast signal transmission in a WDM-PON by using a mutually injected Fabry-Pérot laser diodes," in *Conference Lasers and Electro-Optics*, OSA Technical Digest (Optical Society of America, 2011), paper CFH7.
10. F. Xiong, W. D. Zhong, and H. Kim, "A broadcast-capable WDM-PON based on polarization-sensitive weak-resonant-cavity Fabry-Perot laser diodes," *J. Lightwave Technol.* **30**(3), 355–361 (2012).
11. G.-R. Lin, H.-L. Wang, G. C. Lin, Y. H. Huang, Y. H. Lin, and T. K. Cheng, "Comparison on injection-locked FabryPerot laser diode with front-facet reflectivity of 1% and 30% for optical data transmission in WDM-PON system," *J. Lightwave Technol.* **27**(14), 2779–2785 (2009).
12. G. R. Lin, Y. S. Liao, Y. C. Chi, H. C. Kuo, G. C. Lin, H. L. Wang, and Y. J. Chen, "Long-cavity Fabry-Perot laser amplifier transmitter with enhanced injection-locking bandwidth for WDM-PON application," *J. Lightwave Technol.* **28**(20), 2925–2932 (2010).
13. G.-R. Lin, Y. H. Lin, C. J. Lin, Y. C. Chi, and G. C. Lin, "Reusing a data-erased ASE carrier in a weak-resonant-cavity laser diode for noise-suppressed error-free transmission," *IEEE J. Quantum Electron.* **47**(5), 676–685 (2011).
14. Y. C. Chi, Y. C. Li, H. Y. Wang, P. C. Peng, H. H. Lu, and G. R. Lin, "Optical 16-QAM-52-OFDM transmission at 4 Gbit/s by directly modulating a coherently injection-locked colorless laser diode," *Opt. Express* **20**(18), 20071–20077 (2012).
15. Y. S. Liao, Y. C. Chi, H. C. Kuo, and G. R. Lin, "Pulsating master and injected slave weak-resonant-cavity laser diodes based quasi-color-free 2.5Gb/s RZ DWDM-PON," in *Optical Fiber Communication Conference*, OSA Technical Digest (Optical Society of America, 2011), paper JWA67.
16. G.-R. Lin, T. K. Cheng, Y.-C. Chi, G. C. Lin, H. L. Wang, and Y. H. Lin, "200-GHz and 50-GHz AWG channelized linewidth dependent transmission of weak-resonant-cavity FPLD injection-locked by spectrally sliced ASE," *Opt. Express* **17**(20), 17739–17746 (2009).
17. D. Wulich, "Definition of efficient PAPR in OFDM," *IEEE Commun. Lett.* **9**(9), 832–834 (2005).
18. H. G. Myung and D. J. Goodman, in *Single carrier FDMA: a new air interface for long term evolution*, X. Shen and Y. Pan ed. (Wiley, New York, 2008).
19. S. Sivaprakasam and R. Singh, "Gain change and threshold reduction of diode laser by injection-locking," *Opt. Commun.* **151**(4-6), 253–256 (1998).
20. Y. C. Chang, Y. H. Lin, J. H. Chen, and G.-R. Lin, "All-optical NRZ-to-PRZ format transformer with an injection-locked Fabry-Perot laser diode at unloading condition," *Opt. Express* **12**(19), 4449–4456 (2004).
21. G.-R. Lin, Y. H. Lin, and Y. C. Chang, "Theory and experiments of a mode-beating noise-suppressed and mutually injection-locked Fabry-Perot laser diode and erbium-doped fiber amplifier link," *IEEE J. Quantum Electron.* **40**(8), 1014–1022 (2004).
22. S. Daumont, B. Rihawi, and Y. Lout, "Root-raised cosine filter influences on PAPR distribution of single-carrier signals," in *Proceedings of IEEE Conference on International Symposium Computer Science Society* (Institute of Electrical and Electronics Engineers, New York, 2008), pp. 841–845.
23. G. R. Lin, Y. C. Chi, Y. S. Liao, H. C. Kuo, Z. W. Liao, H. L. Wang, and G. C. Lin, "A pulsed weak-resonant-cavity laser diode with transient wavelength scanning and tracking for injection-locked RZ transmission," *Opt. Express* **20**(13), 13622–13635 (2012).

1. Introduction

With the demand of broadband services increases rapidly to cater various customer applications, the Full Service Access Network (FSAN) group has been discussing actively the next-generation passive optical network (NG-PON1 and NG-PON2) to provide higher bandwidth economically [1]. PONs using wavelength-division multiplexing (WDM) have been widely deliberated to be a viable candidate for NG-PON2. Since colorless optical network units (ONUs) are essential for WDM-PONs, numerous components injected by a centralized light source have been proposed to develop colorless transmitters for uplink [2–10]. In addition, a colorless transmitter is expected to meet some additional requirements, such as low cost, wide wavelength coverage and high data rate. Recently, reflective semiconductor optical amplifier (RSOA) has been demonstrated to provide wide wavelength coverage of more than 60 nm [5,6]; nonetheless, the cost of RSOAs is one of the weaknesses that need to address for the stringent requirement of high anti-reflection (AR) coating (reflectance $< 10^{-3}$), which is essential to increase modulation bandwidth. As an alternative colorless solution, injection-locked Fabry-Perot laser diode (FPLD) has been proposed to offer a cost-effective solution. The etalon effect of an FPLD, however, will limit the wavelength injection-locking range and the gain spectral bandwidth [11,12]. To release the

etalon effect and the AR-coating requirement simultaneously, a weak-resonant-cavity FPLD (WRC-FPLD) has been proposed as a compromise [10,13,14]. With relaxed AR-coating requirement of ~1% reflectance, the WRC-FPLD maintains cost-effectiveness and provides not only wider gain spectral bandwidth, but also better tolerance to wavelength lock-in range than a standard FPLD [14,15]; hence, WRC-FPLD facilitates the injection-locking condition. The modulation bandwidth of the above components, including the WRC-FPLD, is still limited to several GHz; therefore, using conventional on-off keying (OOK) that has low spectral efficiency, the uplink data rates of these directly-modulated colorless devices are only in the range of 155 Mbps ~5 Gbps [10,11,16]. Thanks to the advance in digital-signal-processing (DSP) technology, orthogonal frequency-division multiplexing (OFDM)-PON has been envisioned as a prominent alternative for using higher order quadrature amplitude modulation (QAM) format that improves spectral efficiency effectively, along with decreasing the bandwidth requirement of components ultimately. However, one vital disadvantage of OFDM scheme: the relatively high peak-to-average-power ratio (PAPR) [17,18], which causes nonlinear distortion, higher quantization noise, less power budget and higher amplifier power back-off. Single-carrier frequency domain equalization (SC-FDE) scheme has retained most of advantages of OFDM, such as simple one-tap frequency domain equalization, high bandwidth efficiency, and tolerance to inter-symbol interference (ISI) with simply adding cyclic prefix (CP); moreover, SC-FDE scheme has lower PAPR than OFDM [18].

In this work, we have demonstrated the uplink signals at the mode of 1560.7 nm, 1545.3 nm and 1574.7 nm using the WRC-FPLD; consequently, the results show similar performances in above three cases and the feasibility to support at least 36 WDM channels. For OFDM scheme, we have experimentally demonstrated a 20-Gbps OFDM signals transmission using the power-loading technique over 25-km standard single mode fiber (SSMF). For the SC-FDE scheme, we also have demonstrated 20-Gbps SC-FDE transmission over 25-km SSMF, consequently, SC-FDE scheme shows a better performance than OFDM owing to lower PAPR. The effective data throughputs are 17.9 Gbps excluding CP and training symbols (TS) for both OFDM and SC-FDE signals. Table 1 compares the state-of-art transmitter performances based on injection-locked FPLDs or WRC-FPLD in WDM-PONs. We have achieved highest data rate up to 20 Gbps with modulation of high spectral efficiency, and extended supported channels to 36 with using the WRC-FPLD.

Table 1. State-of-the-art injection-locked schemes based on FPLDs or WRC-FPLDs in WDM-PONs

	SIT ⁷	AO ⁸	KAIST ⁹	NTU ¹⁴	This work
Data rate (Gb/s)	2.5	1.25	2.5	4	20
Distance (km)	8	20	20	25	25
# of channel (wavelength nm)	-	32	10	-	36
Transmitter	FPLD	FPLD	FPLD	WRC-FPLD	WRC-FPLD
Modulation format	OOK	OOK	OOK	OFDM	OFDM/SC-FDE
Year of publication	2009	2011	2011	2012	2013

2. WRC-FPLD configuration and characteristics

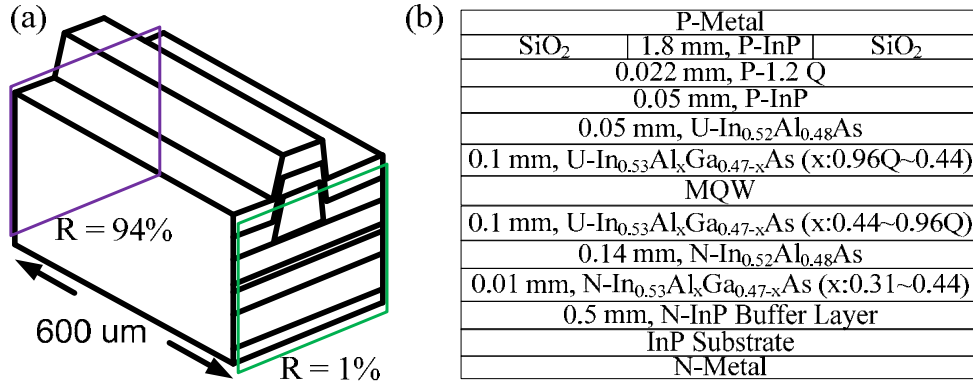


Fig. 1. (a) The ridge-waveguide structure and (b) configuration parameters of the employed WRC-FPLD.

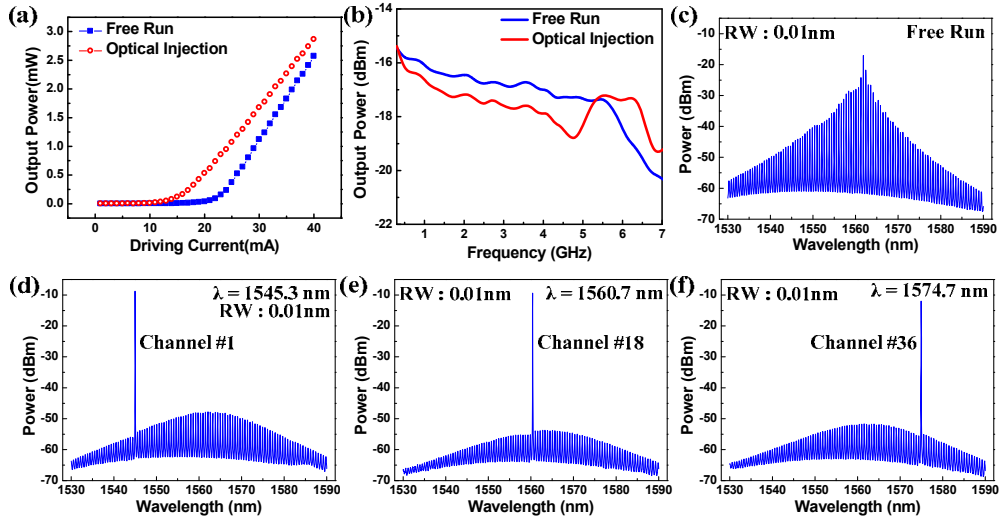


Fig. 2. (a) L-I curve and (b) frequency response of WRC-FPLD for free run and optical injection. (c) Optical spectrum of free-running WRC-FPLD. (d) Optical spectra of the WRC-FPLD injected by a CW with the wavelength of 1545.3 nm, (e) 1560.7 nm, and (f) 1574.7 nm.

The WRC-FPLD is designed with a typical ridge-waveguide structure consisting of a multi-quantum-well active layer as illustrated in Fig. 1(a); the cavity length of the device is 600 μm ; the reflectance of 1% of front-end facet is chosen to retain partial injection-locking of the WRC-FPLD. The parameters of configuration are depicted in Fig. 1(b). In characteristic measurements, the threshold current of WRC-FPLD is 20 mA in free run and reduces to 15 mA with injection light [19,20] as shown in Fig. 2(a). Figure 2(b) shows the frequency responses of the directly modulated WRC-FPLD without and with external injection-locking and reveals that the modulation bandwidth slightly increases from 6 to 6.5 GHz. Additionally, injection locking further induces a frequency dip at 5 GHz is also observed. Not only the negative slope of the injection-locked WRC-FPLD frequency response is slightly increased, but also the output power of the directly modulated WRC-FPLD is attenuated to degrade the throughput. Accordingly, the effects of the increased driving current and the enlarged injection level compensate each other. This is mainly attributed to the strong injection-locking which preserves the wavelength and coherence but degrades the throughput of the WRC-

FPLD. Figure 2(c) depicts the optical spectrum of 0.01-nm resolution when the driving current is 40 mA at 25°C, along with the longitudinal mode spacing of 0.55 nm is observed. Figures 2(d)-2(f) illustrate the optical spectra of the WRC-FPLD injected by -5-dBm CW laser of 1543.5 nm, 1560.7 nm and 1574.7 nm, respectively; the side mode suppression ratio (SMSR) of three cases are all over 40 dB [21]. We also demonstrate a 36-channel supported transmission from wavelength of 1545.3 to 1574.7 nm using WRC-FPLD which exhibits channel spacing of 68.75 GHz.

3. Experimental setup and results

We have demonstrated uplink transmission using the injected WRC-FPLD with OFDM and SC-FDE scheme. The OFDM and SC-FDE schemes have many similarities in block diagram as shown in Fig. 3. For instance, both OFDM and SC-FDE requires CP to overcome inter-symbol interference (ISI) issue and discrete Fourier transform (DFT) for frequency domain equalization. The only one dissimilarity between the OFDM and SC-FDE schemes is the location of the inverse discrete Fourier transform (IDFT) block. The transmitter of SC-FDE scheme is simpler than the OFDM scheme; therefore, for the uplinks of WDM-PONs, the SC-FDE scheme is more practical than the OFDM scheme, for the complexity of SC-FDE at ONUs is lower than OFDM. Moreover, SC-FDE signal retains the advantages of OFDM and provides an additional strength of low PAPR. In this work, the parameters of the OFDM signal includes: inverse fast Fourier transform (IFFT) size of 512, CP of 1.5%, TS of 9%, modulation format of 32 QAM, and subcarrier number of 205, which corresponds to around 4-GHz bandwidth. Likewise, the parameters of the SC-FDE signal includes: CP of 1.5% and TS of 9%, modulation format of 32-QAM, symbol rate of 4-GSymbol/s; additionally, SC-FDE signal is shaped by a square-root-raised-cosine filter with the roll-off factor of 0.1 and a bandwidth of 2.2 GHz, then, the complex signal is upconverted to 2.2 GHz to be real. The effective data throughputs are 17.9 Gbps excluding CP and TS for both OFDM and SC-FDE signals. Without considering the overhead of CP and TS, both OFDM/SC-FDE signals yield data rate of up to 20 Gbps. Figure 3 shows that OFDM needs IDFT at transmitter, but SC-FDE scheme does not; accordingly, the complexity of SC-FDE scheme at ONUs is reduced. Moreover, The OFDM signal is the combination of all subcarriers. When more subcarriers are in phase for some input data, the signal would have higher peak power; contrarily, SC-FDE signal is based on conventional single carrier scheme signal except it adopts equalization in frequency domain. Figure 4 shows the complementary cumulative distribution function (CCDF) curves of PAPR of the OFDM and SC-FDE signals; $\Pr(\text{PAPR} > \text{PAPR}_0)$ denote the probability that PAPR is higher than PAPR_0 [18,22]. The PAPR of the OFDM signal is about 6 dB higher than that of the SC-FDE signal in the simulation of Fig. 4, in fact high PAPR of the signal can severely affect the performance in our experiment.

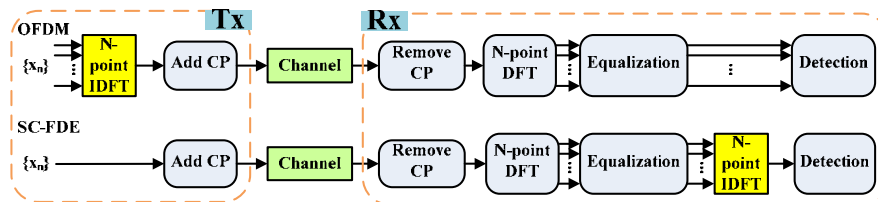


Fig. 3. Block diagrams of OFDM and SC-FDE schemes.

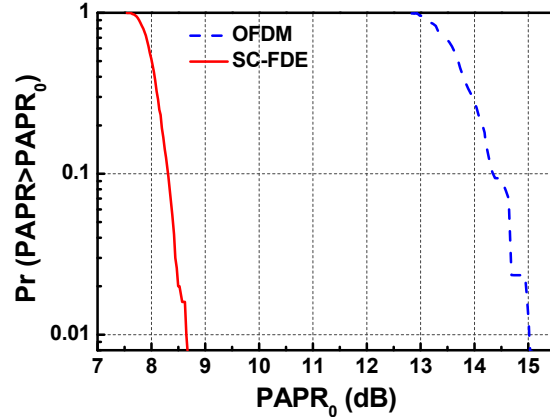


Fig. 4. Comparison of CCDF of PAPR for OFDM and SC-FDE signals.

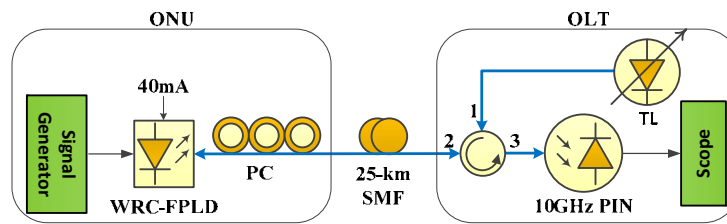


Fig. 5. Experimental setup of OFDM and SC-FDE transmissions.

Figure 5 depicts the experimental setup schematically, and the transmitter at each ONU is composed of a colorless WRC-FPLD, which is injected by a centralized CW light source sent from a tunable laser (TL) at the optical light termination (OLT). Remarkably, the CW light sources at the OLT can be shared by several different WDM-PONs to reduce the cost. The OFDM/SC-FDE signals are generated using Matlab[®] programs, and the electrical driving signals are then carried out by an arbitrary waveform generator (AWG, Tektronix[®] AWG7122) with the sampling rate of 10 GS/s and the digital-to-analog conversion resolution of 8 bits. The driving current of WRC-FPLD is set to two-time threshold current of 40 mA, and the laser temperature is regulated at 25°C. The injection CW power is optimized to -5 dBm at the wavelength of 1560.7 nm, 1545.3 nm and 1574.7 nm, for minimizing power budget and operating up to 20 Gbps at the same time. The wavelength detuning range has been optimized to acquire highest SMSR, which will achieve lowest BER [23]. The optical modulation index has been optimized by maximizing the electrical output signal power of signal generator, since we do not use the electrical power amplifier at ONUs for cost reduction. Afterwards, the WRC-FPLD is modulated directly by the OFDM/SC-FDE signals. After 25-km SSMF transmission, the direct detection is performed by a 10-GHz PIN diode. Next, the received electrical signals are captured and digitized by an oscilloscope (Tektronix[®] DPO71254) with a sample rate of 50 GS/s and a 3-dB bandwidth of 12.5 GHz. The demodulation is performed with the off-line Matlab[®] DSP programs. For OFDM demodulation, after removing CP, the time-domain OFDM signals are transformed into frequency-domain signals by DFT with fast Fourier transform (FFT) size of 512 to implement frequency-domain equalization and hard decision. For SC-FDE demodulation, first, the SC-FDE signals are downconverted to baseband and subsequently filtered by a square-root-raised-cosine filter with roll-off factor 0.1. Second, resemble the demodulation process of OFDM, frequency-domain equalization is implemented after removing CP and executing

DFT of FFT size of 512. The frequency-domain SC-FDE signals are transformed into time-domain signals again by IDFT before implementing hard decision.

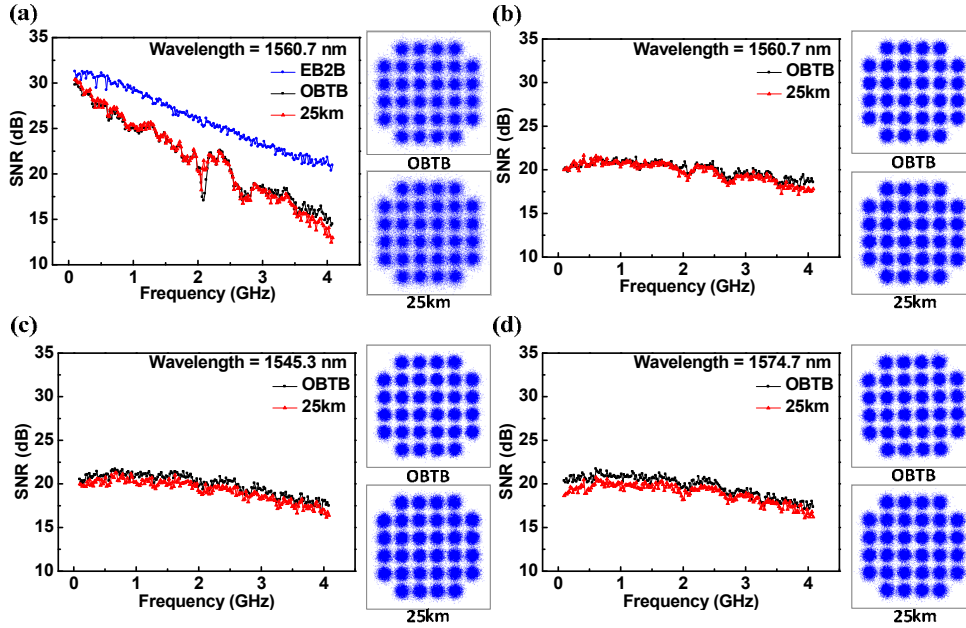


Fig. 6. (a) SNR of OFDM signal of electrical back-to back, optical back-to-back and 25-km SSMF transmission before power-loading at injection wavelength of 1560.7 nm. SNR of OFDM signal of optical back-to-back and 25-km SSMF transmission after power-loading at injection wavelengths of (b) 1560.7, (c) 1545.3, and (d) 1574.7 nm.

Figure 6 shows the signal-to-noise ratio (SNR) of the OFDM signals of electrical back-to-back, optical back-to-back and after 25-km SSMF transmission. The SNR is measured from the constellation to evaluate the bit error rate (BER). The SNR at higher frequency degrades due to the insufficient response of the WRC-FPLD as shown in Fig. 6(a), of which the injection wavelength and the received power are 1560.7 nm and -6 dBm, respectively. The subcarriers with low SNR will dominate the system performance; therefore, the power-loading technique is used to enhance the response of higher frequency of WRC-FPLD. Figures 6(b)-6(d) show the SNR of the OFDM signals after power-loading with the received power of -6 dBm, along with the injection wavelength of 1560.7, 1545.3, and 1574.7 nm, respectively. Figures 6(b)-6(d) also show the maximum SNR penalty is around 2 dB after 25-km SSMF transmission. The constellations of each case are illustrated on the right sides of Figs. 6(a)-6(d). Figures 7(a) and 7(b) show the constellations of 20-Gbps SC-FDE signals with injection wavelength of 1560.7 nm at optical back-to-back and after 25-km SSMF transmission, respectively. Figures 7(c)-7(f) show the constellations of SC-FDE signals with injection wavelengths of 1545.3 and 1574.7 nm over SSMF transmission, respectively. The received power of all the signals shown in Fig. 7 is -6 dBm. Figures 8(a)-8(c) show the comparison between the BERs of the OFDM signals and SC-FDE signals after 25-km SSMF transmission; the BERs of the OFDM signals are under the FEC limit of 3.8×10^{-3} at received power of -6.5 dBm for the three cases (injection wavelength of 1560.7, 1545.3, and 1574.7 nm). This implies that all the 36 channels between 1545.3 and 1574.7 nm, which can support at least 20-Gbps OFDM uplink. Figures 8(a)-8(c) also show that the BER can be significantly improved with using SC-FDE scheme, for the low PAPR. Consequently, in addition to OFDM, SC-FDE can be viewed as another promising candidate in WDM-PONs.

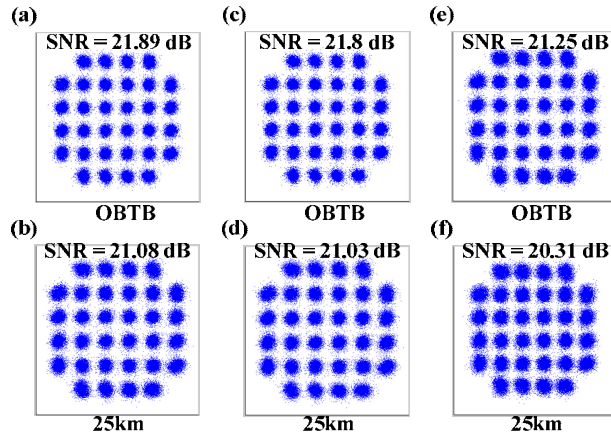


Fig. 7. Constellations of SC-FDE signals at optical back-to-back with injection wavelength of (a) 1560.7, (c) 1543.3 and (e) 1574.7 nm, and those after 25-km SSMF transmission with injection wavelength of (b) 1560.7, (d) 1543.3 and (f) 1574.7 nm.

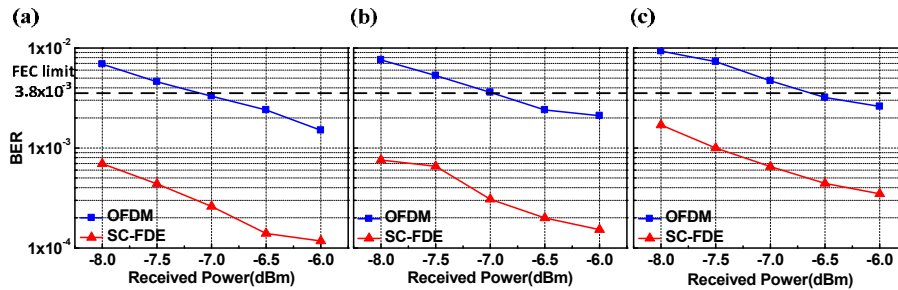


Fig. 8. Receiver sensitivities of OFDM and SC-FDE after 25-km SSMF transmission with injection wavelength of (a) 1560.7, (b) 1545.3, and (c) 1574.7 nm.

4. Conclusion

We have experimentally demonstrated optical OFDM and SC-FDE over 25-km SSMF transmission by using a cost-effective WRC-FPLD, and the FEC limit is achieved for both modulation schemes. While the wavelengths of uplink signals are controlled by centralized injection, the WRC-FPLD-based ONUs are colorless in a WDM-PON. Moreover, owing to the advantage of lower PAPR, the SC-FDE signals outperform the OFDM signals with the fixed 32-QAM format in the proposed system; accordingly, SC-FDE can be another promising candidate for WDM-PONs. Furthermore, the performance of three cases (injection wavelength of 1560.7, 1545.3, and 1574.7 nm) resemble each other. Consequently, we have demonstrated up to 36 channels supported using the WRC-FPLD with the mode spacing of 0.55 nm in the WDM-PON.